



Excitation Transfer from Cr²⁺ to Fe²⁺ Ions in Co-doped ZnSe as a Pumping Scheme for Infrared Solid-State Lasers

Jens W. Tomm¹ · Günter Steinmeyer¹ · Pia Fürtjes¹ · Uwe Griebner¹ · Thomas Elsaesser¹

Received: 8 November 2022 / Accepted: 3 May 2023 / Published online: 26 May 2023
© The Author(s) 2023

Abstract

We present the results of the photoluminescence behavior reflecting Cr²⁺ → Fe²⁺ excitation transfer in co-doped ZnSe:Cr²⁺Fe²⁺. This transfer can be seen as a possible promising pump mechanism to create short pulse lasers for the 3- to 6- μm wavelengths that can be excited using inexpensive 2- μm pump light sources. In addition to the kinetics, emphasis was put on comparing the intensities of both emissions, those of Cr²⁺ and Fe²⁺. With resonant excitation of Cr²⁺, the kinetics of the Fe²⁺ emission shows a very clear picture of the transfer with 60-ns rise time and the peak delayed by 200 ns. However, the evaluation of the PL intensities brought a surprise. With efficiencies above 80%, the observed Cr²⁺ → Fe²⁺ transfer is much more efficient than theoretically expected, and even the overall efficiency including the losses at the Fe²⁺ ions of almost 4% is still an order of magnitude higher than the theoretical values given for the Förster transfer alone. This leads to the suspicion that either the dopant atoms might not be uniformly distributed in the samples or that the transfer mechanism might be more effective than previously thought.

Keywords II–VI semiconductor · co-doped ZnSe · ZnSe:Cr²⁺Fe²⁺ · excitation transfer · kinetics · Förster transfer · laser

Introduction

Cr²⁺ and Fe²⁺ defect centers located at Zn-sites in the zincblende lattice of ZnSe exhibit broad emission bands at 2.4 μm and 4.5 μm , respectively.^{1,2} Therefore, such classical II–VI semiconductor crystals appear ideal candidates for optically pumped solid-state lasers in the mid-infrared range. In particular, the phonon-broadened character of the emission bands is appealing for building mid-infrared mode-locked lasers with few-cycle pulse duration (see Fig. 1). Therefore, ZnSe:Cr²⁺ has frequently been dubbed as the Ti:sapphire of the mid-infrared. While commercial high-power Tm-doped fiber lasers are conveniently available for pumping ZnSe:Cr²⁺ lasers, there are no lasers offering the elevated pump power requirements of ZnSe:Fe²⁺ at 3.2 μm . Given this constraint, direct excitation of Cr²⁺ ions at 2.4 μm with subsequent Cr²⁺ → Fe²⁺ excitation transfer offers a promising alternative. This transfer has been the subject of

several previous studies.^{3–7} Consistently, both experimental and theoretical studies showed such unsatisfactory results for the overall transfer efficiency that a practical use for this mechanism seemed quite unlikely. In a previous study,⁸ however, we observed a six-fold acceleration of the Cr²⁺ photoluminescence (PL) in co-doped ZnSe:Cr²⁺Fe²⁺ compared to a singly-doped reference sample. While this finding is highly suggestive of an efficient transfer process, the overall efficiency was again measured as a meager 3.6%. The aim of current work is the clarification of this apparent contradiction. Covering a wider range of doping concentrations, we augmented our time-resolved PL studies on singly- and co-doped crystals. Analysis of these experimental results confirms our earlier suspicion of a high Cr²⁺ → Fe²⁺ transfer efficiency, pinpointing non-radiative losses of excited Fe²⁺ ions as the source of the relatively poor overall efficiency. Mitigation strategies for practical laser applications involve cooling of the ZnSe:Cr²⁺Fe²⁺ laser crystals.

✉ Jens W. Tomm
tomm@mbi-berlin.de

¹ Max-Born-Institut für Nichtlineare Optik und Kurzzeitspektroskopie, Max-Born-Str. 2A, 12489 Berlin, Germany

Experimental

Our study comprises singly-doped ZnSe:Cr²⁺ and ZnSe:Fe²⁺ as well as co-doped ZnSe:Cr²⁺Fe²⁺ crystals with ion concentrations of $3 \times 10^{16} \text{ cm}^{-3}$... $5.5 \times 10^{18} \text{ cm}^{-3}$, $4 \times 10^{18} \text{ cm}^{-3}$, and $3 \times 10^{16} \text{ cm}^{-3}$... $7.5 \times 10^{18} \text{ cm}^{-3}$. These crystals were purchased from several commercial sources: Egorov Scientific US, 3photon Lithuania, and IPG Photonics US. The sample from the last source are grown by chemical vapor deposition,⁹ while the others are Bridgeman-grown singly crystals. We characterized the samples by standard transmission measurements at ambient temperature. Concentrations (N) of optically active Cr²⁺ and Fe²⁺ ions were determined using the commonly accepted absorption cross-sections of $1.1 \times 10^{-18} \text{ cm}^2$ and $0.97 \times 10^{-18} \text{ cm}^2$ for Cr²⁺ and Fe²⁺ ions, respectively.^{3,10,11}

The transient PL was excited with pulsed lasers, described in detail by Fürtjes et al.¹² Excitation wavelengths were $\lambda_{\text{ex}} = 2.05 \mu\text{m}$ (pulse duration 3 ps) and $\lambda_{\text{ex}} = 3.24 \mu\text{m}$ (pulse duration 1 ps), using a repetition rate of 1 kHz. PL was detected with a LN₂-cooled

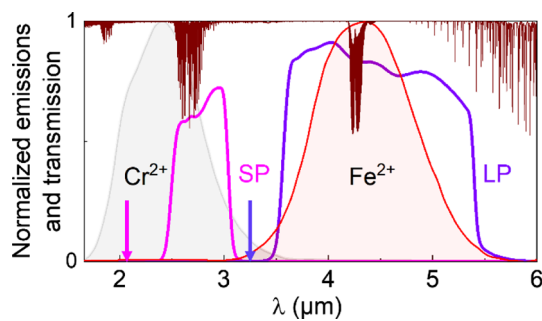
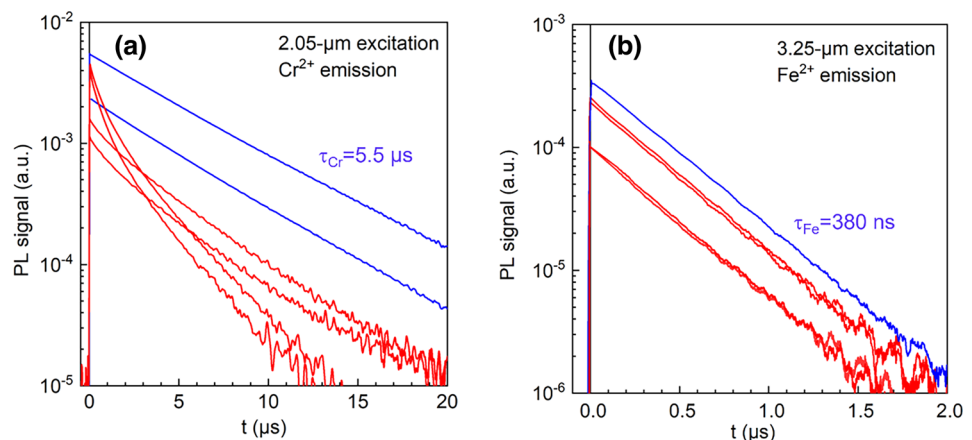


Fig. 1 Normalized emission cross-sections of Cr²⁺ and Fe²⁺ ions in ZnSe³, and the spectral windows used for the investigation (*SP* short pass, *LP* long pass); the *brown line* represents the transmission of 32 cm of air, the path the PL signal has from the sample to the detector (Color figure online)

Fig. 2 PL transients for resonant excitation: (a) from ZnSe:Cr²⁺ and ZnSe:Cr²⁺Fe²⁺ co-doped samples excited $\lambda_{\text{ex}} = 2.05\text{-}\mu\text{m}$ and detected in the *SP* window, (b) from ZnSe:Fe²⁺ and ZnSe:Cr²⁺Fe²⁺ co-doped samples with $3.24\text{-}\mu\text{m}$ excitation and detected in the *LP* window; in (a) and (b), *blue curves* represent data from singly doped samples while data from co-doped samples are given in *red* (Color figure online)



InSb-photodiode (Infrared Acc. ID413), enabling 7-ns temporal resolution. Using a Femto DHPA-100 amplifier with 1-kV/A transimpedance, this temporal resolution remains almost preserved, i.e., we yielded sub-10-ns temporal resolution. Data recording was by a 4-GHz oscilloscope (DPO 70404C; Tektronix).

Emission intensities were extracted in spectral windows, named *SP* and *LP*, which are defined by sets of filters (Spectrogon; Edmund Optics). Figure 1 shows them together with the λ_{ex} (arrows) and the normalized emission cross-sections of the Cr²⁺ and Fe²⁺ ions. Although absolute PL intensities cannot be measured, accurate consideration of the excitation, transfer, and detection conditions allows for relative comparison of the PL from the Cr²⁺ and Fe²⁺ ions in terms of photon numbers. In all the experiments, the time-averaged excitation power was set to $\sim 35 \text{ mW}$, avoiding saturation excitation in both ion species.

Results and Discussion

Photoluminescence Kinetics

Figure 2 shows selected PL transients for resonant excitation. Under direct excitation, all the Fe²⁺-doped samples with ions in (b) exhibit a singly-exponential PL decay in the *LP* window, whereas the transients of the Cr²⁺-containing samples exhibit different behaviors, measured in the corresponding *SP* window (Fig. 2a). Among the latter, all singly-doped samples show a strictly exponential decay, which is contrasted by the more or less pronounced non-exponential behavior of the co-doped samples. Such deviations from a singly exponential decay is a hallmark of excitation transfer processes.

Before deepening the discussion on Cr²⁺ \rightarrow Fe²⁺ excitation transfer, let us briefly consider relative PL intensities. Under identical excitation conditions, the total PL emission yield of singly-doped Fe²⁺-doped samples is ~ 14 times

lower than that of the Cr^{2+} PL. This finding already sets a constraint of $\eta_{\text{Fe}} \sim 7\%$ for the maximum quantum efficiency of the Fe^{2+} PL. Further confirmation of this rather poor quantum efficiency can be found in the literature, specifically from temperature-dependent measurements of the PL decay time,^{13–17} indicating the practical absence of the temperature-quenching effects for the Cr^{2+} PL. While the PL decay time (τ_{PL}) of the Cr^{2+} ions remains nearly constant,¹³ the pronounced decrease of τ_{PL} of the Fe^{2+} ions from $\sim 100 \mu\text{s}$ (at $\sim 100 \text{ K}$) to ambient temperature by more than two orders of magnitude can be seen^{14–17} As temperature-quenching is always indicative of non-radiative decay processes, this gives rise to the observed degradation of the PL quantum efficiency of the Fe^{2+} ions.

Figure 3 shows τ_{PL} versus doping concentration, N , as obtained from the transients shown in Fig. 2. In the following discussion, we refer to the inter-ionic distance, R , which is shown as the top abscissa of Fig. 2 and is related to N via $R = (1/N)^{1/3}$. As our sample set covers only a limited doping concentration range, we have additionally included literature data^{3,16,18,19} in Fig. 3. Both ion species exhibit concentration-quenching, i.e., excitation transfer between ions of identical species. However, the quenching effects only appear for $N > 10^{19} \text{ cm}^{-3}$, giving rise to a reduction of τ_{PL} . As our studies only comprised samples of lower doping, we can therefore safely rule out concentration-quenching. In agreement with previous reports,

we also find that, in co-doped samples, the respective other dopant reduces the PL decay time of the studied species;^{3,4,18,20,21} compare positions of squares (singly-doped) and circles (co-doped) in both parts. The observed τ_{PL} reductions with N are empirically described by:

$$\tau_{\text{PL}} = \frac{\tau_{\text{Cr,Fe}}}{1 + \left(\frac{N_{\text{Cr,Fe}}}{N_0}\right)} \quad (1)$$

see, e.g.,¹⁶ where N_0 is a fit parameter quantifying the concentration quenching threshold. The respective values $N_0 = 4 \times 10^{19} \text{ cm}^{-3}$ and $1.07 \times 10^{20} \text{ cm}^{-3}$ for Cr^{2+} and Fe^{2+} indicate that this process starts at lower doping levels for Cr^{2+} . In addition, the general shape of this calculated curve agrees less well with the data points, in contrast to Fe^{2+} , where the calculation and experiment are in better agreement. Overall, this analysis of the PL decay times provides remarkable agreement with data from the literature.

Figure 4 shows PL transients from heavily co-doped sample ($N_{\text{Cr}} = 6.7 \times 10^{18} \text{ cm}^{-3}$, $N_{\text{Fe}} = 6.1 \times 10^{18} \text{ cm}^{-3}$) after $\lambda_{\text{ex}} = 2.05\text{-}\mu\text{m}$ excitation taken in the SP and LP windows. Extra measurements served to exclude a contribution of directly excited Fe^{2+} ions, making us conclude that the LP transient has its origin in the radiative recombination from Fe^{2+} ions that have been indirectly excited via Cr^{2+} ions. This assertion is confirmed by.

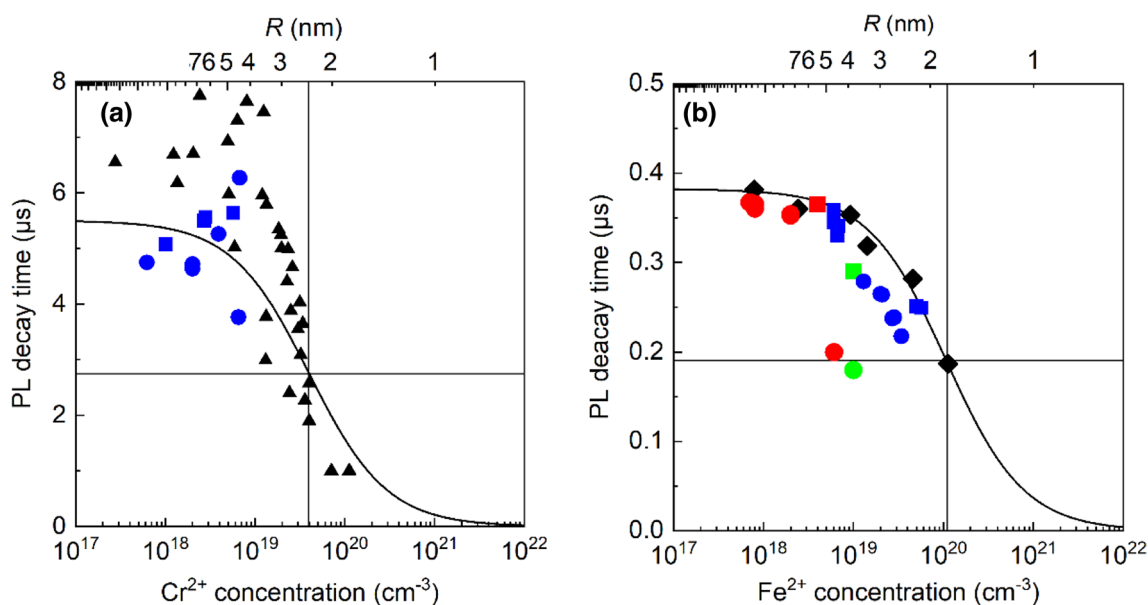


Fig. 3 PL decay time versus ion concentrations for resonant excitation: (a) $\lambda_{\text{ex}} = 2.05 \mu\text{m}$ and detection in the SP window; *blue symbols* stem from fits to transients in the 10.0- to 12.5- μs temporal window (see Fig. 2a), *black symbols* are taken from figure 5 in Ref. 19 and see Refs. 13,27 (b) $\lambda_{\text{ex}} = 3.24 \mu\text{m}$ and detection in the LP window; *red*

symbols are from fits to transients in the 0.25- to 1.0- μs temporal window (see Fig. 2(b); *black, blue, and green symbols* are data from Refs. 16, 4, and 3, respectively. In (a) and (b), *squares and circles* represent data from singly- and co-doped samples, respectively (Color figure online)

- The rise time (~ 60 ns) of the transient, which substantially exceeds the time resolution (< 10 ns),
- a delayed peak some 200 ns after the excitation laser peak, and
- a significantly increased PL decay time of the Fe²⁺ PL of ~ 1 μ s.

These experimental findings can be accurately explained by a rate equation model, which will be presented elsewhere.²² Qualitatively, the complex time evolution of the

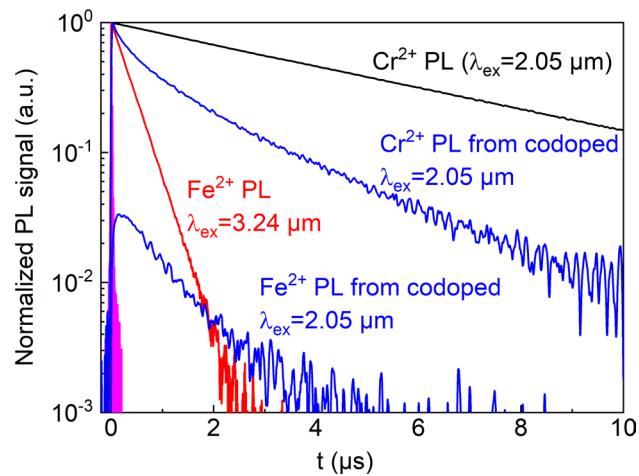


Fig. 4 Normalized PL transients from 3 samples; *blue transients* show the PLs from a heavily co-doped sample ($N_{\text{Cr}} = 6.7 \times 10^{18} \text{ cm}^{-3}$, $N_{\text{Fe}} = 6.1 \times 10^{18} \text{ cm}^{-3}$) after $\lambda_{\text{ex}} = 2.05$ - μm excitation taken in the SP and LP windows; *black and red curves* serve for reference and have been obtained from singly-doped samples (Color figure online)

Fe²⁺ PL originates from a distribution of excitation transfer times, arising from a distribution of transfer distances in the ZnSe host crystal. At the shortest distances, the fastest processes result in the initial increase of the Fe²⁺ PL with a 60-ns rise time, while slower transfer processes cause Fe²⁺ ions to emit light much beyond their intrinsic PL decay time of 380 ns.

Photoluminescence Intensities

Apart from direct analysis of PL kinetics, it also appears interesting to compare the time-integrated PL intensities of the two ion species in co-doped samples for an estimation of the transfer efficiency. Figure 4 shows an example case, with an integrated intensity ratio of 1:0.03, i.e., the luminous efficiency of the Fe²⁺ ions is 33 times lower than that of the Cr²⁺ ions. Recalling that the radiative quantum efficiency is less than $\eta_{\text{Fe}} = 7\%$, one concludes that the Cr²⁺ \rightarrow Fe²⁺ excitation transfer must be relatively efficient, with a value of $\eta_{\text{Transfer}} = 83\%$ for this particular sample. Figure 5 shows integrated intensity ratios of the two ion species versus Fe²⁺ concentration. For our most heavily Fe²⁺-doped sample ($N_{\text{Cr}} = 6.5 \times 10^{18} \text{ cm}^{-3}$, $N_{\text{Fe}} = 7.5 \times 10^{18} \text{ cm}^{-3}$), we even conclude a transfer efficiency of $\eta_{\text{Transfer}} = 87\%$.

In the light of the previously discussed poor overall efficiency, nearly perfect transfer efficiencies appear highly surprising. In the consistent view of the literature on Förster transfer, dipole–dipole interaction appears as the key mechanism. The original publications by Förster²³ and Dexter²⁴ are summarized by Henderson and Imbusch,²⁵ and were applied to the material system discussed here by Fedorov et al.³ Based on this theoretical approach, Doroshenko

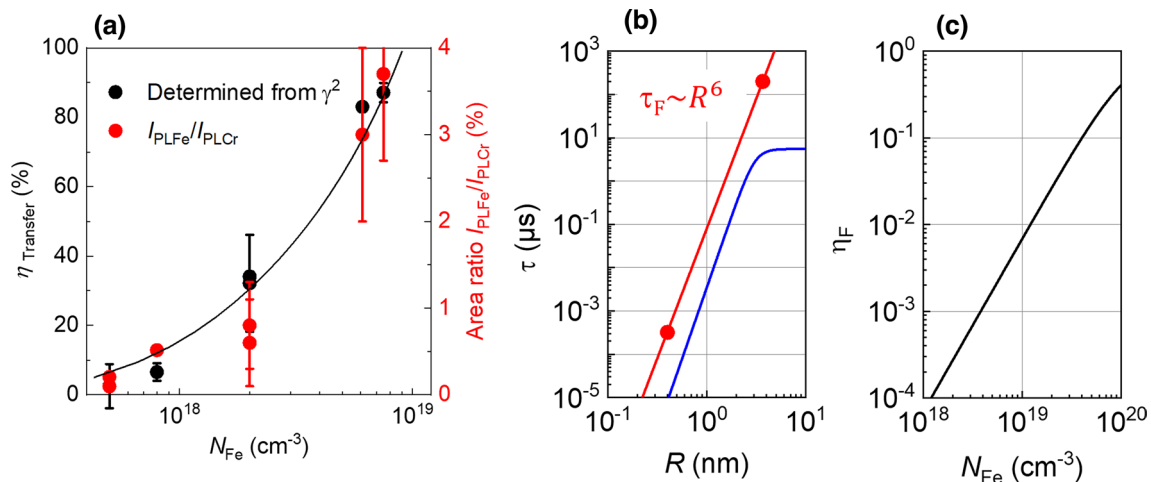


Fig. 5 (a) Cr²⁺ \rightarrow Fe²⁺ excitation transfer efficiency calculated from γ according to Doroshenko et al.²⁶; the *right ordinate* shows the integrated PL intensity ratios of Fe²⁺ to Cr²⁺ PLs for the same samples (see *full red circles*); the *black line* is a guide for the eye. (b) Förster transfer time (τ_{F}) according to Fedorov et al.³ (*red line*) and expected

PL decay time taking into account τ_{F} and $\tau_{\text{Cr}} = 5.5$ μ s (see Fig. 2a); see *blue line* versus interionic spacing; the *full red circles* are from table 1 in Fedorov et al.³ (c) Förster transfer efficiency $\eta_{\text{F}} = \tau_{\text{Cr}} / (\tau_{\text{Cr}} + \tau_{\text{F}})$ versus Fe²⁺ concentration (Color figure online)

et al.²⁶ estimated a similar high transfer efficiency of $\eta_{\text{Transfer}} = 53\text{--}55\%$ by analyzing the Cr^{2+} PL in their $\text{Zn}_{1-x}\text{Mn}_x\text{Se}:\text{Cr}^{2+}\text{Fe}^{2+}$ samples. Specifically, the authors separated exponential and non-exponential contributions to their Cr^{2+} transients, and plotted the non-exponential part versus the square root of time. The slopes, γ , obtained from the linear fits of the data enabled an alternative method for estimating efficiencies. In order to verify our above conclusions, we also followed this approach, as shown in Fig. 5a with respect to the left ordinate.

Finally, we compared our PL decay times with the calculations by Fedorov et al.³ Figure 5b and c shows the time constants and the resulting η_{Transfer} , respectively. Considering the latter, we find that, even for our most heavily Fe^{2+} -doped sample ($N_{\text{Fe}} = 7.5 \times 10^{18} \text{ cm}^{-3}$), Fedorov's calculations suggest a value of $\eta_{\text{Transfer}} < 0.3\%$ (see Fig. 5c), i.e., a discrepancy of two orders of magnitude that mandates further clarification. To this end, we see two different approaches to resolving this discrepancy. On the one hand, all discussion so far has assumed a homogeneous distribution of ions in the ZnSe host, i.e., all Zn sites are populated by Cr^{2+} and Fe^{2+} with the same probability. An inhomogeneous ion distribution with clustered interionic distances would result in higher rates of excitation transfer. On the other hand, enhancement of the transfer rates could also arise from phonon-assisted processes. Future work is required to resolve this remaining open question.

Conclusions

For our study of the transfer efficiency, both singly-doped crystals and six co-doped $\text{ZnSe}:\text{Cr}^{2+}\text{Fe}^{2+}$ crystals were studied using time-resolved PL spectroscopy. In addition to the kinetics, great emphasis was placed on measuring and comparing the intensities of both PLs, from Cr^{2+} and Fe^{2+} . The kinetics of the Cr^{2+} and Fe^{2+} emissions in the different crystals show a consistent pattern. In particular, when we resonantly excite the co-doped samples in the Cr^{2+} absorption band, we find clear indications for an efficient excitation transfer from Cr^{2+} to Fe^{2+} , including a rapid initial rise time (~ 60 ns) of the transient, a delayed peak of about 200 ns after the peak of the excitation laser, and finally a significantly prolonged PL decay time of the Fe^{2+} PL of $\sim 1 \mu\text{s}$. Given the short 380-ns lifetimes of the Fe^{2+} ions, the latter finding can only be explained by replenishment via the $\text{Cr}^{2+} \rightarrow \text{Fe}^{2+}$ transfer process. Careful analysis of the PL measurements revealed a surprising finding, i.e., with efficiencies above 80%, the observed $\text{Cr}^{2+} \rightarrow \text{Fe}^{2+}$ transfer is much more efficient than theoretically expected. Accounting for non-radiative losses of Fe^{2+} , even the overall efficiency is still an order of magnitude higher than estimated by Fedorov et al.³ Finally, mitigation of excessive non-radiative losses of

the Fe^{2+} ions may be addressed by carefully adapted cooling of the co-doped laser crystals. If this remaining challenge can be solved, we are very optimistic about the $\text{Cr}^{2+} \rightarrow \text{Fe}^{2+}$ transfer, enabling a useful pumping scheme for short-pulse mid-infrared laser sources.

Acknowledgments We appreciate helpful discussions with Stanislav Balabanov, Oleg Pronin, Nazar Kovalenko, and Daniel Többsen. Technical support from Sandy Schwirzke-Schaaf and Janett Feickert is gratefully acknowledged.

Author's Contributions JWT and TE designed the research. PF and JWT carried out the TRPL experiment. PF, UG and JWT constructed the setup. GS conducted data analysis. All authors contributed to the discussion of the results and the manuscript.

Funding Open Access funding enabled and organized by Projekt DEAL. This work has received funding from the European Union's Horizon 2020 research and innovation program under Grant agreement No. 871124 Laserlab-Europe.

Availability of Data and Material Data underlying the results presented in this paper are not publicly available at this time but may be obtained from the authors upon reasonable request.

Conflict of interest The authors declare that there is no conflict of interest regarding the content of this article.

Consent to Participate All authors are agreed.

Open Access This article is licensed under a Creative Commons Attribution 4.0 International License, which permits use, sharing, adaptation, distribution and reproduction in any medium or format, as long as you give appropriate credit to the original author(s) and the source, provide a link to the Creative Commons licence, and indicate if changes were made. The images or other third party material in this article are included in the article's Creative Commons licence, unless indicated otherwise in a credit line to the material. If material is not included in the article's Creative Commons licence and your intended use is not permitted by statutory regulation or exceeds the permitted use, you will need to obtain permission directly from the copyright holder. To view a copy of this licence, visit <http://creativecommons.org/licenses/by/4.0/>.

References

1. E. Sorokin, S. Naumov, and I.T. Sorokina, Ultrabroadband infrared solid-state lasers. *IEEE J. Sel. Top. Quantum Electron.* 11, 690 (2005).
2. T. Irina, Sorokina and Evgeni Sorokin, femtosecond Cr^{2+} -based lasers. *IEEE J. Select. Top. Quantum Electron.* 21, 1601519 (2015).
3. V. Fedorov, T. Carlson, and S. Mirov, Energy transfer in iron-chromium co-doped ZnSe middle-infrared laser crystals. *Opt. Mater. Express* 9, 2340 (2019).
4. V.A. Antonov, K.N. Firsov, E.M. Gavrishchuk, V.B. Ikonnikov, I.G. Kononov, T.V. Kotereva, S.V. Kurashkin, S.V. Podlesnykh, S.A. Rodin, D.V. Savin, A.A. Sirotkin, A.M. Titireenko, and N.V. Zhavoronkov, Luminescent and lasing characteristics of polycrystalline $\text{Cr}:\text{Fe}:\text{ZnSe}$ excited at 2.09 and 2.94 μm wavelengths. *Laser Phys. Lett.* 16(9), 095002 (2019). <https://doi.org/10.1088/1612-202X/ab3851>.

5. J. Peppers, V.V. Fedorov, and S.B. Mirov, Mid-IR photoluminescence of Fe²⁺ and Cr²⁺ ions in ZnSe crystal under excitation in charge transfer bands. *Opt. Express* 23, 4406 (2015).
6. T. Carlson, O. Gafarov, V. Fedorov, and S. Mirov, *Presented at the Laser Congress 2018 (ASSL)* (Boston: Massachusetts, 2018). (**unpublished**).
7. X.Y. Wang, Z. Chen, L. Zhang, B. Jiang, Xu. Min, J. Hong, Y. Wang, P. Zhang, L. Zhang, and Y. Hang, Preparation, spectroscopic characterization and energy transfer investigation of iron-chromium diffusion co-doped ZnSe for mid-IR laser applications. *Opt. Mater.* 54, 234 (2016).
8. P. Fürtjes, J.W. Tomm, U. Griebner, G. Steinmeyer, S.S. Balabanov, E.M. Gavrishchuk, and T. Elsaesser, Kinetics of excitation transfer from Cr²⁺ to Fe²⁺ ions in co-doped ZnSe. *Opt. Lett.* 47, 2129 (2022).
9. <https://www.ipgphotonics.com/en/products/components/mid-ir-crystals>
10. J.W. Evans, B.D. Dolasinski, T.R. Harris, J.W. Cleary, and P.A. Berry, Demonstration and power scaling of an Fe:CrMnTe laser at 52 microns. *Opt. Mater. Express* 7(3), 860 (2017). <https://doi.org/10.1364/OME.7.000860>.
11. S.B. Mirov, V.V. Fedorov, D. Martyshekin, I.S. Moskalev, M. Mirov, and S. Vasilyev, Progress in mid-IR lasers based on Cr and Fe-doped II–VI chalcogenides. *IEEE J. Select. Top. Quantum Electron.* 21(1), 292–310 (2015). <https://doi.org/10.1109/JSTQE.2014.2346512>.
12. P. Fuertjes, L. von Grafenstein, D. Ueberschaer, C. Mei, U. Griebner, and T. Elsaesser, Compact OPCPA system seeded by a Cr:ZnS laser for generating tunable femtosecond pulses in the MWIR. *Opt. Lett.* 46, 1704 (2021).
13. L.D. DeLoach, R.H. Page, G.D. Wilke, S.A. Payne, and W.F. Krupke, Transition metal-doped zinc chalcogenides: spectroscopy and laser demonstration of a new class of gain media. *IEEE J. Quantum Electron.* 32, 885 (1996).
14. J.J. Adams, C. Bibeau, R.H. Page, D.M. Krol, L.H. Furu, and S.A. Payne, 4.0–4.5- μm lasing of Fe:ZnSe below 180 K, a new mid-infrared laser material. *Opt. Lett.* 24, 1720 (1999).
15. V.V. Fedorov, S.B. Mirov, A. Gallian, D.V. Badikov, M.P. Frolov, Y.V. Korostelin, V.I. Kozlovsky, A.I. Landman, Y.P. Podmar'kov, V.A. Akimov, and A.A. Voronov, 3.77–5.05- μm tunable solid-state lasers based on Fe²⁺-doped ZnSe crystals operating at low and room temperatures. *IEEE J. Quantum Electron.* 42(9), 907–917 (2006). <https://doi.org/10.1109/JQE.2006.880119>.
16. NoSung Myoung, V.V. Fedorov, S.B. Mirov, and L.E. Wenger, Temperature and concentration quenching of mid-IR photoluminescence in iron doped ZnSe and ZnS laser crystals. *J. Lumin.* 132, 600 (2012).
17. M.E. Doroshenko, H. Jelínková, M. Jelínek, D. Vyhliđal, J. Šulc, N.O. Kovalenko Šulc, and I.S. Terzin, Influence of the pumping wavelength on laser properties of Fe²⁺ ions in ZnSe crystal. *Opt. Lett.* 44(7), 1686 (2019). <https://doi.org/10.1364/OL.44.001686>.
18. M. Surma, M. Godlewski, and T.P. Surkova, Iron and chromium impurities in ZnSe as centers of nonradiative recombination. *Phys. Rev. B* 50, 8319 (1994).
19. A. Burger, K. Chattopadhyay, J.O. Ndap, X. Ma, S.H. Morgan, C.I. Rablau, C.H. Su, S. Feth, R.H. Page, K.I. Schaffers, and S.A. Payne, Preparation conditions of chromium doped ZnSe and their infrared luminescence properties. *J. Cryst. Growth* 225, 249 (2001).
20. M. Godlewski, M. Surma, V.Y. Ivanov, and T.P. Surkova, Mechanisms of radiative and nonradiative recombination in ZnSe: Cr and ZnSe:Fe. *Low Temp. Phys.* 30, 891 (2004).
21. I. Radevici, K. Sushkevich, G. Colibaba, V. Sirkeli, H. Huhtinen, N. Nedeoglo, D. Nedeoglo, and P. Paturi, Influence of chromium interaction with native and impurity defects on optical and luminescence properties of ZnSe: Cr crystals. *J. Appl. Phys.* 114, 203104 (2013).
22. G. Steinmeyer, J.W. Tomm, P. Fuertjes, U. Griebner, S.S. Balabanov, and T. Elsaesser, Efficient electronic excitation transfer via phonon-assisted dipole-dipole coupling in Fe²⁺:Cr²⁺:ZnSe. *Phys. Rev. Appl.* 19, 054043 (2023).
23. T. Förster, Experimentelle und theoretische Untersuchung des zwischenmolekularen Übergangs von Elektronenanregungsenergie. *Z. Nat. A* 4, 321 (1949).
24. D.L. Dexter, A theory of sensitized luminescence in solids. *J. Chem. Phys.* 21, 836 (1953).
25. B. Henderson and M. Imbusch, *Optical Spectroscopy of Inorganic Solids* (Oxford: Oxford Science Publications, 2006), p.445.
26. M.E. Doroshenko, H. Jelinkova, A. Riha, M. Jelinek, M. Nemeč, N.O. Kovalenko, and A.S. Gerasimenko, Mid-IR (44 μm) Zn_{1-x}Mn_xSe:Cr²⁺, Fe²⁺ (x = 0.3) laser pumped by 17 μm laser using Cr²⁺-Fe²⁺ energy transfer. *Opt. Lett.* 44, 2724 (2019).
27. R.H. Page, K.I. Schaffers, L.D. DeLoach, G.D. Wilke, F.D. Patel, J.B. Tassano, S.A. Payne, W.F. Krupke, K.T. Chen, and A. Burger, Cr²⁺-doped zinc chalcogenides as efficient, widely tunable mid-infrared lasers. *IEEE J. Quantum Electron.* 33, 609 (1997).

Publisher's Note Springer Nature remains neutral with regard to jurisdictional claims in published maps and institutional affiliations.